Plant Cell Physiol. 46(6): 975–984 (2005)
doi:10.1093/pcp/pci106, available online at www.pcp.oupjournals.org

The Lysine-rich Arabinogalactan-protein Subfamily in *Arabidopsis*: Gene Expression, Glycoprotein Purification and Biochemical Characterization

Wenxian Sun [1, 3, 4], Jianfeng Xu [2], Jie Yang [1, 3], Marcia J. Kieliszewski [2, 3] and Allan M. Showalter [1, 3, 5]

[1] *Department of Environmental and Plant Biology, Ohio University, Athens, OH 45701-2979, USA*
[2] *Department of Chemistry and Biochemistry, Ohio University, Athens, OH 45701-2979, USA*
[3] *Molecular and Cellular Biology Program, Ohio University, Athens, OH 45701-2979, USA*

***AtAGP17*, *AtAGP18* and *AtAGP19* are homologous genes encoding three putative glycosylphosphatidylinositol (GPI)-anchored classical arabinogalactan-proteins (AGPs) in *Arabidopsis*. They are distinguished from other AGPs by a short, C-terminal lysine-rich region. Organ-specific expression of these genes was revealed by Northern blot analysis. *AtAGP17* was strongly expressed in leaves and stems, and weakly expressed in flowers and roots; *AtAGP18* was strongly expressed in flowers, and moderately expressed in roots, stems and young leaves; and *AtAGP19* was strongly expressed in stems, moderately expressed in flowers and roots, and weakly expressed in young leaves. One of these genes, *AtAGP17*, was expressed and purified as a green fluorescent protein (GFP) fusion protein in transgenic tobacco cells using hydrophobic interaction chromatography, size exclusion chromatography and reverse phase high-performance liquid chromatography. The fusion (glyco)protein produced a characteristic AGP 'smear' with a molecular mass of 80–150 kDa when detected by Western blot analysis. Glycosyl composition and linkage analyses of purified GFP–AtAGP17 showed that carbohydrate accounted for ~86% of the molecule, with arabinose and galactose as major, and rhamnose and glucuronic acid as minor glycosyl residues and with 1,3,6-galactose, 1,4-glucuronic acid, 1,3-galactose and terminal arabinose as major linkages. GFP–AtAGP17 was also precipitated by β-Yariv reagent, further confirming that AtAGP17 is a *bona fide* AGP. Confocal fluorescence microscopy of plasmolysed, transformed cells indicated that AtAGP17 is localized on the plasma membrane and in Hechtian strands. Hydroxyproline (Hyp) glycoside profiles of GFP–AtAGP17 in conjunction with the deduced protein sequence also served to corroborate the Hyp contiguity hypothesis, which predicts contiguous Hyp residues as attachment sites for arabinosides and clustered, non-contiguous Hyp residues as attachment sites for arabinogalactan polysaccharides.**

Keywords: *Arabidopsis* — Arabinogalactan-proteins — Glycoprotein — Hydroxyproline.

Abbreviations: AG, arabinogalactan; AGP, arabinogalactan-protein; Gal*p*, galactopyranose; GFP, green fluorescent protein; GPI, glycosylphosphatidylinositol; HRGPs, hydroxyproline-rich glycoproteins; Hyp, hydroxyproline; RP HPLC, reverse-phase high performance liquid chromatography.

Introduction

Arabinogalactan-proteins (AGPs) are a family of hyperglycosylated, cell surface hydroxyproline (Hyp)-rich glycoproteins (HRGPs) found throughout the plant kingdom. AGPs are broadly implicated to function in different aspects of plant growth and development, such as cell proliferation, cell expansion, cell differentiation, cell-cell recognition, somatic embryogenesis, pollen tube growth and programmed cell death (McCabe et al. 1997, Nothnagel 1997, Showalter 2001). However, few studies have assigned the precise function(s) to particular AGPs. Functional studies of AGPs are hindered because of the limited number of well-characterized AGPs, especially on a glycoprotein level.

Completion of the *Arabidopsis* genome project (Arabidopsis Genome Initiative 2000) has facilitated identification of 50 putative AGPs from the *Arabidopsis* database, most of which await biochemical verification and analysis in order to address the functional goals of the Arabidopsis 2010 project (Schultz et al. 2002). In *Arabidopsis*, these putative AGPs are divided into at least five subfamilies: 14 classical AGPs with protein backbones harboring classical AGP domains, three classical AGPs containing a short, characteristic lysine-rich subdomain, 12 AG peptides with short, peptide backbones of 10–15 amino acid residues, 21 fasciclin-like AGPs, and an unknown number of non-classical AGPs, which are difficult to discover via database searches because of the lack of easily identifiable protein characteristics (Borner et al. 2002, Schultz et al. 2002, Borner et al. 2003).

AtAGP17, *AtAGP18* and *AtAGP19* encode the three putative classical AGPs distinguished by a C-terminal lysine-rich region. Like many AGPs predicted from the *Arabidopsis* genome, AGPs in the lysine-rich subfamily contain putative glycosylphosphatidylinositol (GPI) attachment signals at their C-termini that may target proteins to the outer surface of the plasma membrane. Biochemical evidence for such GPI-anchored AGPs has emerged only recently. Genomic and pro-

[4] Present address: Department of Plant Pathology, University of Wisconsin-Madison, Madison, WI 53706, USA.
[5] Corresponding author: E-mail, showalte@ohio.edu; Fax, +1-740-593-1130.

teomic analysis of GPI-anchored proteins in *Arabidopis* has revealed that ~40% of these GPI-anchored proteins (totaling 248 in number) are predicted AGPs or proteins containing AGP modules (Youl et al. 1998, Oxley and Bacic 1999, Sherrier et al. 1999, Svetek et al. 1999, Borner et al. 2003, Sun et al. 2004b).

The carbohydrate moiety of AGPs typically accounts for ~90% of the mass of AGPs and consists mainly of arabinose and galactose, although other sugars including uronic acids are frequently present. Two types of carbohydrate can be found attached to the AGP protein backbone, namely type II arabinogalactan polysaccharide chains and short oligoarabinosides, which are covalently bound to non-contiguous and contiguous Hyp residues, respectively (Kieliszewski and Lamport 1994, Kieliszewski et al. 1995). Given the difficulty in purifying native AGPs, much of this information is obtained using bulk or partially purified AGP preparations; however, it is substantiated by carbohydrate analysis of a limited number of purified or highly enriched AGP preparations (Shpak et al. 1999, Zhao et al. 2002).

Although bioinformatics has provided much insight into the AGP gene family in *Arabidopsis*, few AGP structural and functional studies are reported in this model plant. Characterization of a limited number of AGP mutants in *Arabidopsis*, however, is beginning to provide some functional insight. Through such studies, AtAGP17 and AtAGP18 are implicated to function in *Agrobacterium* binding to roots and female gametogenesis, respectively, while a non-classical AGP (AtAGP30) and a fasciclin AGP (AtFLA4) are implicated to function in abscisic acid (ABA) signaling during seed germination and cell-cell adhesion, respectively (Nam et al. 1999, Shi et al. 2003, van Hengel and Roberts 2003, Acosta-Garcia and Vielle-Calzada 2004, Gaspar et al. 2004). In addition, Motose et al. (2004) have identified *Arabidopsis xyp1xyp2* double mutants. *AtXYP1* and *AtXYP2* encode xylogen proteins that contain small AGP modules and function in vascular development. Comparative genomic and genetic analyses provide little information about post-translational modifications of these mature glycoproteins, which undoubtedly play a profound role in AGP functions. Thus, in order to make inroads toward understanding the structure and corresponding function of *Arabidopsis* AGPs, we report here on the members of the lysine-rich classical AGP subfamily, AtAGP17, AtAGP18 and AtAGP19, in terms of their organ-specific expression, and the biochemical purification and characterization of AtAGP17 as a green fluorescent protein (GFP) fusion product.

Results

Analysis of the lysine-rich AGP gene family

AtAGP17, AtAGP18 and AtAGP19 are distinguished from other *Arabidopsis* classical AGPs by a C-terminal lysine-rich region. These proteins share amino acid sequence similarity to the biochemically well-characterized homolog in tomato, LeAGP-1, as well as to other homologs including tobacco NaAGP4, cucumber CsAGP-1 and pine PtaAGP6 (Gao et al. 1999, Gilson et al. 2001, Zhao et al. 2002, Park et al. 2003, Zhang et al. 2003, Sun et al. 2004b) (data not shown). Clustal analysis and the resulting phylogenetic tree of these various lysine-rich AGPs along with other known classical AGPs and AG peptide sequences from *Arabidopsis* show that the lysine-rich AGPs constitute a distinct phylogenetic branch (Fig. 1). Interestingly, while AtAGP17 and AtAGP18 are closely related to one another and to their apparent orthologs in other plant species, AtAGP19 is more distantly related, with no clear orthologous sequences with the possible exception of PtaAGP6.

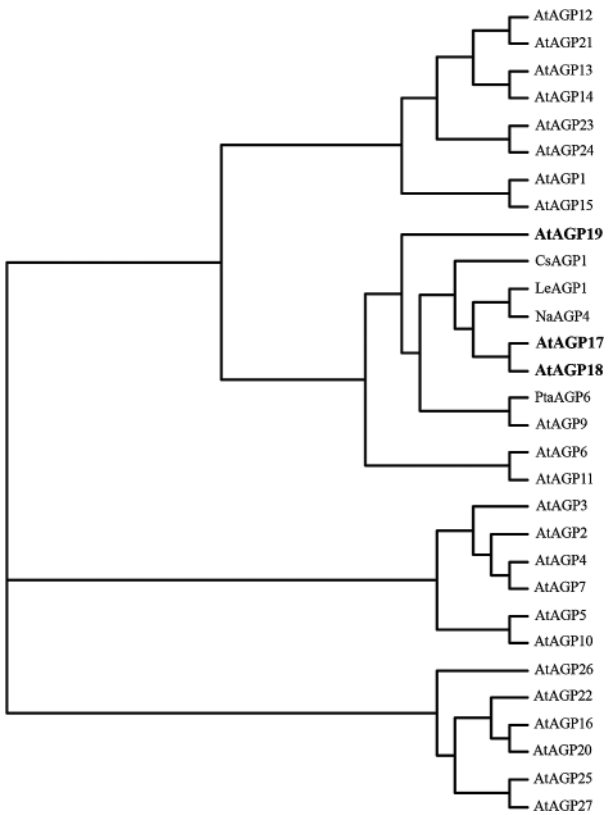

Fig. 1 Phylogenetic tree of classical AGPs, lysine-rich classical AGPs and AG peptides from *Arabidopsis* derived from Clustal X analysis. This tree also includes lysine-rich classical AGPs from tomato (LeAGP-1), tobacco (NaAGP4), cucumber (CsAGP1) and pine (PtaAGP6).

Organ-specific expression patterns of AtAGP17, AtAGP18 and AtAGP19

In order to study which organs express *AtAGP17*, *AtAGP18* and *AtAGP19*, total RNA was extracted from different organs of 1-month-old *Arabidopsis* plants, including young and old leaves, roots, elongated inflorescence stems and flowers, and subjected to Northern blot analysis. Expression of these genes varied in different organs (Fig. 2A). *AtAGP17* was

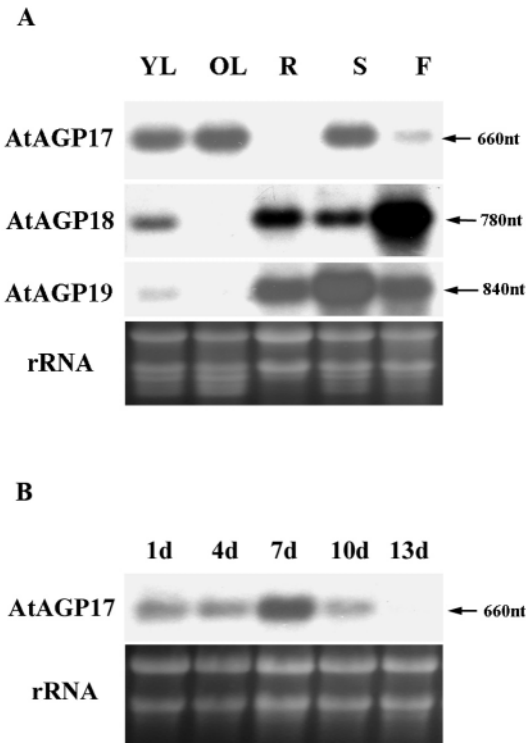

Fig. 2 Northern blot analysis of *AtAGP17*, *AtAGP18* and *AtAGP19* gene expression in different organs of *Arabidopsis* plants and cultured cells. (A) Organ-specific mRNA expression patterns of *AtAGP17*, *AtAGP18* and *AtAGP19*. YL, young leaves; OL, old leaves; R, roots; S, elongating inflorescence stems; F, flowers. (B) *AtAGP17* mRNA expression in *Arabidopsis* cultured cells at different days after subculture. Ethidium bromide staining of rRNA revealed equal loading of RNA samples. Approximate sizes of these AGP mRNAs are shown on the right.

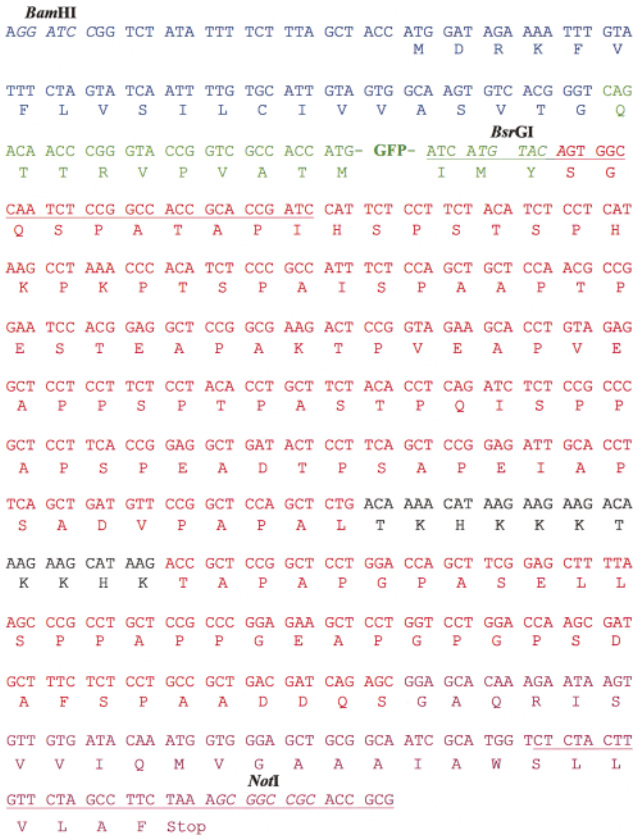

Fig. 3 DNA sequence of *GFP–AtAGP17* and its corresponding amino acid sequence. The LeAGP-1 signal sequence (blue) at the N-terminus of the fusion protein was followed by the GFP sequence (green). The fusion protein was terminated with AtAGP17 protein excluding the signal peptide. The modular structure of AtAGP17 is shown in different colors: alanine-, proline-, serine- and threoine-rich AGP domain in red; the short lysine-rich domain in black; and putative GPI anchor addition sequence in purple. Underlined regions indicate primer sequences, including restriction sites (labeled and in italics), utilized for constructing the pUC-SS^{tom}-GFP-AtAGP17 plasmid.

strongly expressed in leaves and stems, weakly expressed in flowers, and barely expressed in roots. *AtAGP18* was very highly expressed in flowers, strongly expressed in roots and stems and weakly expressed in leaves. Expression of *AtAGP19* was strong in stems, moderate in roots and flowers, and very weak in leaves. In addition, *AtAGP17* expression in *Arabidopsis* suspension-cultured cells was examined and found to increase after 1 week of subculturing, but then decreased thereafter (Fig. 2B).

Selection and identification of suspension-cultured cells transformed with GFP–AtAGP17

The GFP–AtAGP17 genetic construction was delivered into tobacco culture cells through *Agrobacterium*-mediated transformation (Fig. 3). Transformed cells were screened on solid

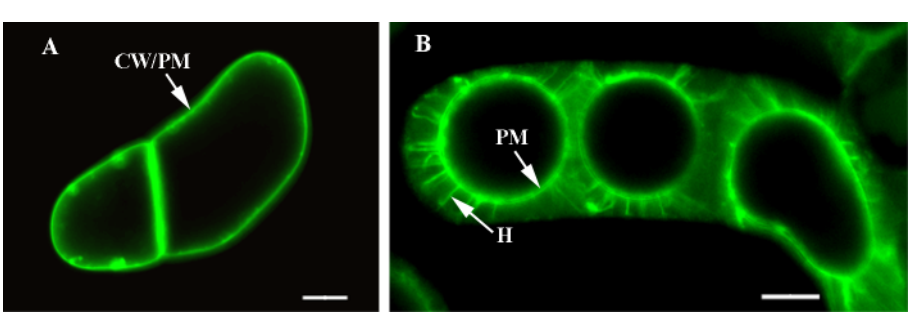

Fig. 4 Transgenic tobacco cells expressing GFP–AtAGP17 before (A) and after (B) plasmolysis. (A) GFP fluorescence was observed at the cell wall–plasma membrane (CW/PM) interface. (B) GFP fluorescence was observed on the plasma membrane (PM) and in Hechtian strands (H), adhesion sites between the plasma membranes and cell walls, after the cells were plasmolysed with 4% NaCl. Bars = 10 μm

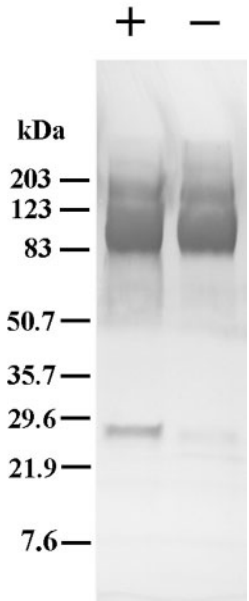

Fig. 5 Western blot analysis of purified GFP–AtAGP17. The fusion protein (10 μg in each well) was separated by SDS–PAGE on a 12% polyacrylamide gel with (+) and without (–) heating in boiling water for 3 min prior to gel loading, electroblotted, and detected with an anti-GFP antibody.

MS or Schenk and Hildebrandt (SH) medium with kanamycin and timentin. After fluorescence microscopic examination, cell lines with the brightest green fluorescence were selected for propagation in liquid culture. Subsequently, cell lines secreting the highest amount of fusion protein into the culture medium were selected and used for further cytochemical and biochemical analysis.

Fluorescence localization of GFP–AtAGP17 fusion protein in transgenic tobacco cells

The subcellular localization of GFP–AtAGP17 in transgenic cells was determined by laser scanning confocal microscopy. Green fluorescence predominantly appeared on the cell surfaces of *GFP–AtAGP17*-transformed cells (Fig. 4A), while untransformed cells showed essentially no background fluorescence, as previously observed (Shpak et al. 1999, Zhao et al. 2002). Moreover, following plasmolysis of these transgenic cells with NaCl, green fluorescence was localized to the retracted plasma membrane and Hechtian strands, which serve as attachment sites between the plasma membrane and cell wall (Fig. 4B).

Purification and characterization of GFP–AtAGP17 fusion protein

In addition to being targeted to the cell surface, GFP–AtAGP17 was also secreted into culture media. The same biochemical strategy used by Zhao et al. (2002) was employed here to purify the GFP–AtAGP17 fusion protein from the conditioned culture medium. By a three-step chromatographic procedure, sequentially involving hydrophobic interaction chromatography, gel filtration chromatography and reverse-phase high-performance liquid chromatography (RP HPLC), the fusion glycoprotein was purified to homogeneity, as indicated by a single symmetric peak after HPLC fractionation (data not shown), and used for biochemical characterization.

Table 1 Amino acid composition of the purified AtAGP17 glycoprotein (following enzymatic removal of GFP) compared with the amino acid compositions deduced from the *AtAGP17* cDNA (TAIR database)

Amino acid	Composition (mol %)	
	AtAGP17 [a]	Purified AtAGP17
Hyp	–	20.8
Pro	27.1	4.3
Asx	3.6	3.2
Thr	8.6	7.8
Ser	13.6	11.3
Glx	7.8	7.9
Gly	3.6	2.8
Ala	17.8	19.9
Val	2.1	3.6
Cys	0.0	0.0
Met	0.0	0.0
Ile	2.8	4.9
Leu	2.1	2.3
Tyr	0.0	0.0
Phe	0.7	0.0
His	2.8	3.0
Lys	7.1	8.4
Arg	0.0	0.0
Trp	0.0	nd

[a] AtAGP17 deduced amino acid sequence excluding the N-terminal signal sequence and the putative GPI anchor addition sequence (TAIR database).
nd, not determined.

The GFP–AtAGP17 fusion protein was subjected to SDS–PAGE and detected by Western blot analysis with an anti-GFP polyclonal antibody. The apparent molecular weight ranged from 80,000 to 150,000 Da (Fig. 5). Heating the fusion protein prior to gel loading caused some GFP to dissociate from the fusion product, consistent with previous reports (Zhao et al. 2002, Sun et al. 2004b). More thorough removal of GFP from the fusion protein, however, was achieved by chymotryptic digestion of a chymotryptic cleavage site (i.e. a tyrosine residue) engineered within the *Bsr*GI restriction site used in creating the transgene (Fig. 3). The carbohydrate moiety of the AtAGP17 glycoprotein covers the protein backbone and protects it from protease cleavage, as was the case for LeAGP-1 examined previously (Zhao et al. 2002). Amino acid composition analysis of AtAGP17 lacking GFP demonstrated that the

Table 2 Glycosyl composition of the AtAGP17 fusion glycoprotein expressed in tobacco

Glycosyl residue	Composition (mol%)
Arabinose	30.1
Galactose	55.1
Glucuronic acid	8.8
Rhamnose	6.0

molar percentages of amino acid residues matched those predicted from the *AtAGP17* gene sequence, with 84% of the proline residues being hydroxylated to Hyp (Table 1).

Glycosyl composition analysis of the GFP–AtAGP17 fusion protein showed that the protein backbone accounted for ~31% of the total mass (i.e. dry weight) of the glycoprotein, while carbohydrate accounted for ~69%. Excluding GFP (~27 kDa), the protein backbone of AtAGP17 (14.3 kDa) accounted for ~14% of the dry weight of the glycoprotein, while carbohydrate accounted for 86%. Glycosyl composition analysis of the fusion protein showed that the major glycosyl residues were arabinose (30.1%) and galactose (55.1%) and the minor components included rhamnose (6.0%) and glucuronic acid (8.8%) (Table 2). In addition, the fusion protein was precipitated by β-Yariv reagent (data not shown).

Hyp glycoside profile analysis of the GFP–AtAGP17 fusion protein showed that 81% of the total Hyp had polysaccharide substituents, while the rest of the Hyp was either not glycosylated (7%) or attached to oligoarabinoses (12%) (Table 3).

Glycosyl linkage analyses of GFP–AtAGP17 and GFP–LeAGP-1 fusion proteins were determined at the Carbohydrate Complex Research Center and at the University of Melbourne, respectively (Table 4). Glycosyl linkages of GFP–LeAGP-1 and GFP–AtAGP17 were consistent with that found in type II arabinogalactans. In particular, the branched 1,3,6-galactopyranose (Gal*p*) linkage was the most abundant linkage, although both 1,3-Gal*p* and 1,6-Gal*p* were also present. Other notable linkages present include an abundance of terminal arabinose residues, particularly in LeAGP-1, with lesser amounts of terminal rhamnose and terminal galactose in both glycoproteins. Both of these glycoproteins also have considerable amounts of 1,4-linked and terminal glucuronic acid. Linkage analysis of GFP–AtAGP17 was generally, but not completely, consistent with the glycosyl composition data. Despite repeating the analysis, linkage analysis underestimated the amount of arabinose present, possibly because of the loss of volatile partially methylated alditol acetate derivatives of arabinose.

Table 4 Glycosyl linkage analysis of GFP–AtAGP17 compared with GFP–LeAGP-1

Glycosyl residues	Percentage	
	GFP–AtAGP17	GFP–LeAGP-1
Terminal-Rha (*p*)	6.5	6.2
Terminal-Ara (*f*)	9.2	22.4
Terminal-Ara (*p*)	3.3	5.8
1,2-Ara (*f*)	0.0	1.7
1,5-Ara (*f*)	0.0	8.3
1,5-Ara (*p*)	4.3	0.0
Terminal-Gal (*p*)	3.3	2.0
1,3-Gal (*p*)	10.5	3.0
1,4-Gal (*p*)	6.2	0.0
1,6-Gal (*p*)	7.6	3.4
1,3 6-Gal (*p*)	28.4	25.5
Terminal-Glc A (*p*)	4.9	4.1
1,4-Glc A (*p*)	15.8	7.6

Rha, rhamnose; Ara, arabinose; Gal, galactose; Glc A, glucuronic acid; p, pyranose; f, furanose.

Discussion

Computer-based searches and analyses of the *Arabidopsis* genome indicate that *AtAGP17*, *AtAGP18* and *AtAGP19*

Table 3 Hyp glycoside profile analysis of GFP–AtAGP17

Hyp glycoside	Experimental % for AtAGP17	Predicted %		
		AtAGP17	AtAGP18	AtAGP19
Hyp-PS	81	~76	~74	~31
Hyp-Ara	3	~12–18 [a]	~16–21 [a]	~56–62 [a]
Hyp-Ara_2	9			
Hyp-Ara_3	0			
Hyp-Ara_4	0			
NG-Hyp	7	~6–12	~5–10	~7–13

Relative amounts of Hyp polysaccharide (Hyp-PS), Hyp arabinosides (Hyp-$Ara_{1–4}$) and non-glycosylated Hyp (NG-Hyp) predicted by the Hyp contiguity hypothesis were compared with experimental data obtained from the purified AtAGP17 fusion glycoprotein. Hyp glycoside profiles predicted for AtAGP18 and AtAGP19 are also included.

[a] These predicted data include the sum of all Hyp arabinosides (i.e. total Hyp-$Ara_{1–4}$).

encode three putative GPI-anchored, classical AGPs distinguished by a short, conserved lysine-rich region (Gilson et al. 2001, Schultz et al. 2002). These AGPs are homologous to the well-characterized tomato LeAGP-1 and to other lysine-rich AGPs from tobacco, cucumber and pine, and constitute a phylogenetically distinct subfamily (Fig. 1). In order to begin to understand the function of this AGP subfamily and complement ongoing functional studies of LeAGP-1, expression patterns of these three *Arabidopsis* AGPs were examined, and one of these AGPs, AtAGP17, was purified to confirm its identity and elucidate its structural and cytochemical properties.

The mRNA expression patterns of *AtAGP17*, *AtAGP18* and *AtAGP19* show that these subfamily members are differentially regulated in an organ-specific manner, providing valuable information to facilitate phenotypic examination of mutants in this gene family (Fig. 2). *AtAGP17* is expressed in leaves and stems, but is not expressed in flowers and roots to any appreciable extent. In contrast, *AtAGP18* is expressed most strongly in flowers, but also in roots, stems and young leaves. This pattern is nearly identical to that reported for *LeAGP-1* and *NaAGP4* (Li and Showalter 1996, Gilson et al. 2001). *AtAGP19* has a similar expression pattern to *AtAGP18*, although it is not as strongly expressed in flowers and young leaves, indicating that these two lysine-rich AGPs may function together. As plants with mutations in these AGP genes are examined to elucidate their functions, these expression data will guide their analysis by indicating where to look for potential phenotypic alterations and which combinations of gene mutants may be required before alterations are observed.

Fluorescence microscopy of GFP–AtAGP17-transformed cells demonstrates that this fusion protein is present at the cell surface where it is found on plasma membranes and in Hechtian strands (Fig. 4). Its localization to the plasma membrane is consistent with the presence of a putative GPI anchor signal sequence predicted from the gene. Furthermore, the subcellular localization of this fusion protein is identical to that of tomato LeAGP-1, which is a confirmed GPI-anchored AGP (Sun et al. 2004b).

As with GFP–LeAGP-1, the GFP–AtAGP17 fusion protein is secreted and readily purified from culture media. The ability to isolate milligram quantities of GFP–AtAGP17 allowed for biochemical characterization of the glycoprotein, including its Hyp glycoside profile as a test of our ability to predict AGP Hyp glycosylation based on the Hyp contiguity hypothesis. Amino acid composition analysis of AtAGP17 (without GFP) is consistent with that predicted from its cDNA sequence and reveals that ~84% of prolyl residues are hydroxylated, as expected for an AGP (Table 1). Western blot analysis indicates that the fusion protein has a molecular mass of 80–150 kDa, consistent with extensive, heterogeneous glycosylation of the polypeptide and with the ~132 kDa average molecular mass calculated for the fusion protein based on glycosyl composition data (Fig. 5, Table 2). Excluding GFP which is not glycosylated (Shpak et al. 1999), the transgenic AtAGP17 has an average molecular mass of ~105 kDa and contains 86% carbohydrate. The fusion glycoprotein contains carbohydrate residues and linkages typical of AGP glycans, consistent with the model in which the type II arabinogalactan polysaccharide consists of a (1→3)-β-D-galactan backbone branched with (1→6)-β-D-galactan side chains (Aspinall 1973, Nothnagel 1997) (Tables 2, 4). In particular, galactose (including 1,3-linked, 1,6-linked, 1,3,6-linked and terminal galactose) and arabinose (1,5-linked and terminal arabinose) represent the major sugar components present, while terminal rhamnose and glucuronic acid (1,4-linked and terminal glucuronic acid) are minor components. The fact that the fusion protein is precipitated by β-Yariv reagent represents additional confirmation that AtAGP17 is a *bona fide* AGP.

To predict Hyp glycosylation of AtAGP17, we turned to the gene, the Hyp contiguity hypothesis and past work (Kieliszewski and Lamport 1994, Shpak et al. 2001). The *AtAGP17* gene encodes a total of 30 non-contiguous proline residues that occur as 11 Ala–Pro, eight Ser–Pro, five Thr–Pro, one Val–Pro, two Lys–Pro and three Gly–Pro and eight contiguous proline residues that occur as two Ala–Pro–Pro and two Ser–Pro–Pro, excluding the N- and C-terminal signal sequences. Based on previous work, we know that the proline residues in the sequences Gly–Pro and Lys–Pro remain non-hydroxylated in HRGPs and probably remain as five proline residues in AtAGP17 (Kieliszewski and Lamport 1994, Goodrum et al. 2000). Thus we predict that there are 33 Hyp residues in AtAGP17; 25 are non-contiguous and eight are contiguous. From the Hyp contiguity hypothesis, we predict that the 25 non-contiguous Hyp residues, or 76% of the total Hyp (25 out of 33 residues), are sites of arabinogalactan polysaccharide addition. The Hyp contiguity hypothesis considered in light of earlier work with a repetitive Ser–Hyp–Hyp sequence (Shpak et al. 2001) predicts that somewhat more than half of the contiguous Hyp residues in Ser–Hyp–Hyp and probably in Ala–Hyp–Hyp as well are arabinosylated (~4–6 out of 33 Hyp residues) and that almost half of the contiguous Hyp remains non-glycosylated (~2–4 residues). These predictions are consistent with the experimentally determined values shown in Table 3 and correspond to the Hyp *O*-glycosylation model of AtAGP17 presented in Fig. 6A. We used a similar approach to predict and model the Hyp glycosylation profile of AtAGP18 (Table 3 and Fig. 6B).

Predictions for Hyp glycosylation of AtAGP19, however, are more difficult because we lack experimentally determined Hyp glycosylation profiles for *Arabidopsis* HRGPs containing X-Hyp/Pro_3 motifs. This motif is common in *Arabidopsis* but rare in the well-characterized solanaceous HRGPs, and it is not a good substrate for solanaceous prolyl hydroxylases. Earlier work with synthetic genes expressed in *Nicotiana* demonstrated that unlike repetitive Ser–Pro_4 and Ser–Pro_2 sequences which are extremely common repeats in solanaceous HRGPs, each proline residue in repetitive Ser–Pro_3 sequences was incompletely hydroxylated, leading to both contiguous and

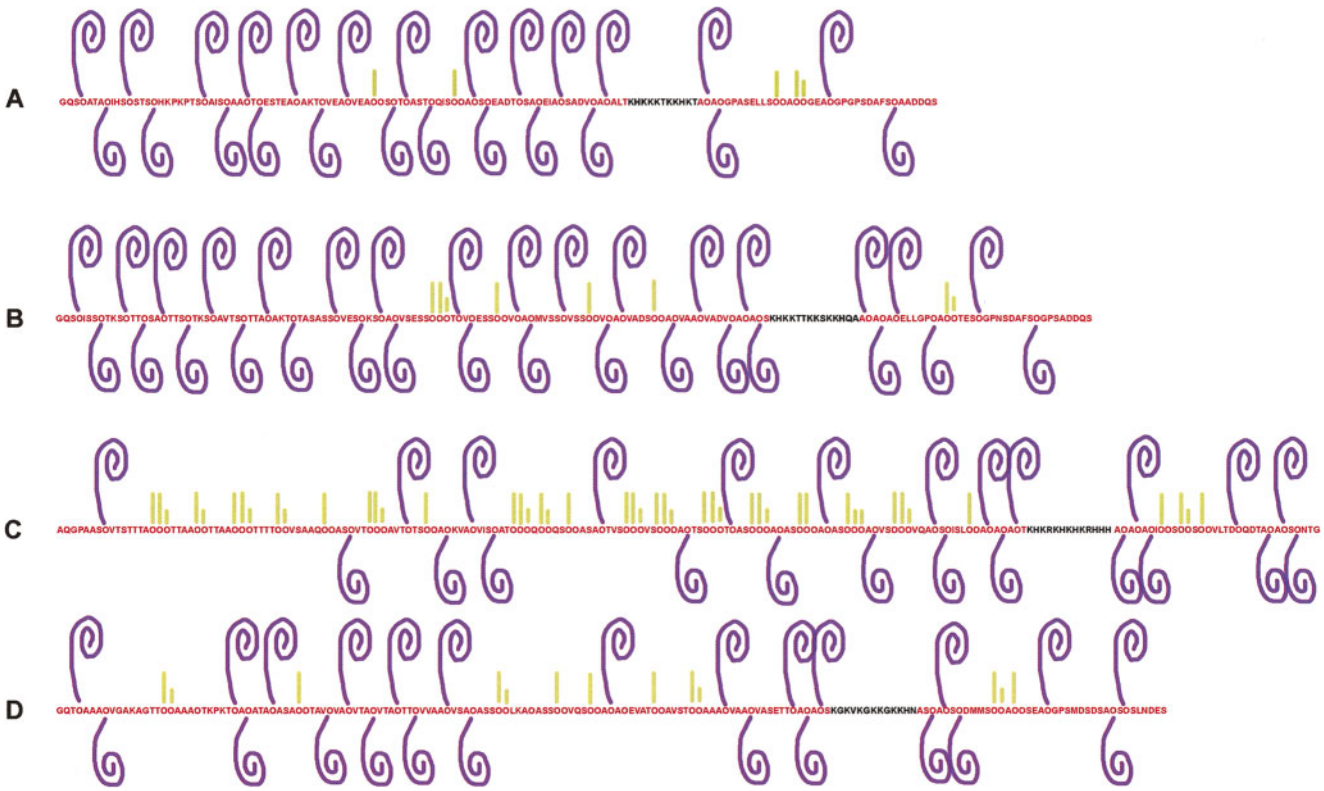

Fig. 6 Proposed models for *O*-Hyp glycosylation of AtAGP17 (A), AtAGP18 (B) and AtAGP19 (C) compared with that of tomato LeAGP-1 (D). Purple spirals represent arabinogalactan polysaccharides; green rods represent arabinosides. The highly basic, lysine-rich module of these proteins is highlighted in black.

non-contiguous Hyp in the polypeptide. Not surprisingly, the resulting glycoprotein contained both Hyp-arabinosides and Hyp-arabinogalactan polysaccharides (Shpak et al. 2001).

However, different species possess prolyl hydroxylases having slightly different specificities tailored to the HRGPs of that species. For example, an HRGP isolated from maize contained Ser–Hyp_3 and Ala–Hyp_3 repeats that serve exclusively as sites of Hyp *O*-arabinosylation (Kieliszewski et al. 1992). Thus, although the Ser–Pro_3 sequence in tobacco is inconsistently hydroxylated, it might be completely hydroxylated in *Arabidopsis*; the hydroxylation pattern of the proline residues would influence the type of Hyp glycosylation of those sequences.

Arabidopsis HRGP genes that clearly encode extensins (Merkouropoulos et al. 1999) and presumably therefore have Hyp arabinosylation but not polysaccharide addition to Hyp, contain abundant Ser–Pro_3 repeats in addition to Ser–Pro_4 repeats, for example as part of the larger P2 extensin-type repeat Ser–$Pro_{3–4}$-VYK (Smith et al. 1986). However, Ser–Pro_3-containing extensins in *Arabidopsis* have yet to be biochemically characterized and so we can only speculate that the *Arabidopsis* AtAGP19 Xaa–Pro–Pro–Pro repeats are all hydroxylated and subsequently arabinosylated. Assuming this, we propose the AtAGP19 Hyp glycosylation profile shown in Table 3 and the corresponding glycoprotein Hyp *O*-glycosylation model presented in Fig. 6C. These proposed glycosylation models for AtAGP17–19 were also compared with that of tomato LeAGP-1 (Fig. 6D) (Zhao et al. 2002) and show that AtAGP19 is unique with respect to its greater number of arabinosides. Furthermore, while the biological consequences of these glycosylation patterns are unknown at present, these extensive modifications, which define most of the interactive molecular surface of these AGPs, will need to be reconciled with the undoubtedly critical roles which they play in determining their molecular interactions and functions. Likewise, the role of the conspicuously non-glycosylated lysine-rich region in molecular interactions and functions remains to be elucidated despite one line of experimentation that indicates that this region may be important for normal fruit and seed development (Sun et al. 2004a).

The purification and structural characterization of AtAGP17, as well as LeAGP-1, now allow for studies of molecular interactions with these AGPs, and provide a basis for functional examination of these AGPs, particularly in transgenic and mutant plants where expression of these AGPs is altered. For instance, the resistant to *Agrobacterium* transformation (*rat1*) mutant is an *Arabidopsis* T-DNA insertion line with the tag in the *AtAGP17* promoter (Nam et al. 1999, Gaspar

et al. 2001, Gaspar et al. 2004); this insertion apparently does not totally inactivate the gene. Given that AtAGP17 is barely expressed in wild-type *Arabidopsis* roots, it is difficult to reconcile this information with the *rat1* phenotype of reduced binding of *Agrobacterium* in roots. As *rat1* and other *AtAGP17* mutant plants are identified and characterized more completely, the structural and regulatory information of this AGP presented here will be valuable in designing experiments and ultimately in understanding its function.

Materials and Methods

Plant materials

Arabidopsis (ecotype Columbia) plants were grown at 23°C under a 15 h/9 h (light/dark) cycle. Tobacco (*Nicotiana tobacum* BY-2) cells were cultured in SH medium (Sigma, St Louis, MO, USA) and *Arabidopsis* cells were cultured in Gamborg's B5 medium (Sigma) on a rotary shaker (120 rpm) at 26°C.

Construction of plasmid pUC-SS^{tom}-EGFP-AtAGP17

A *Bsr*GI restriction site was introduced to the 5′ end of *AtAGP17* (TAIR database) immediately after the signal sequence, and a *Not*I restriction site was introduced to the 3′ end of *AtAGP17* via polymerase chain reaction (PCR) amplification (Fig. 3). The 5′ sense primer containing the *Bsr*GI site (underlined) was 5′-ATC ATG TAC AGT GGC CAA TCT CCG GCC ACC GCA CCG ATC-3′, and the 3′ antisense primer containing the *Not*I site (underlined) was 5′-CGC GGT GCG GCC GCT TTA GAA GGC TAG AAC AAG TAG AG-3′. The amplified *AtAGP17* fragment was cloned into plasmid *pUC-SS^{tom}-GFP-LeAGP-1* (Zhao et al. 2002) as a *Bsr*GI–*Not*I fragment in place of the *LeAGP-1* cDNA sequence. The new construct was designated as *pUC-SS^{tom}-GFP-AtAGP17* and was sequenced at the Ohio University DNA sequencing facility. After sequencing, the construct was subcloned into the plant vector pBI121 (Clontech, Palo Alto, CA, USA) as a *Bam*HI–*Sac*I fragment in place of the glucuronidase reporter gene with the 35S cauliflower mosaic virus (CaMV) promoter left behind to drive expression.

Agrobacterium and tobacco cell transformation and selection of cell lines

The pBI121-based plasmid harboring the *GFP–AtAGP17* construct was delivered into *Agrobacterium tumefaciens* strain LBA4404 by the freeze–thaw method (An et al. 1988). *Agrobacterium*-mediated cell transformation and selection and maintenance of transformed tobacco cell lines were conducted as described by Zhao et al. (2002). Transgenic cells were subcultured every 2–3 weeks in SH medium.

Confocal laser scanning fluorescence microscopy

Expression of the GFP–AtAGP17 fusion protein in transgenic tobacco cells was observed using a Zeiss confocal laser scanning fluorescence microscope LSM510 with a GFP filter set (Zeiss, Germany).

Purification of GFP–AtAGP17

Purification of the GFP–AtAGP17 fusion protein was performed according to the procedure described by Shpak et al. (1999) with minor modifications. Briefly, conditioned medium was collected from 14- to 18-day-old transgenic tobacco cell suspension cultures, concentrated by rotary evaporation and dialyzed with distilled water. NaCl was added to concentrated cell medium to achieve a final concentration of 2 M, and then the medium was loaded on a phenyl-Sepharose 6 Fast Flow column (16×700 mm, Amersham Pharmacia Biotech Piscataway, NJ, USA), previously equilibrated in 2 M NaCl. The column was sequentially eluted with 1 M NaCl and distilled water. The fluorescent fraction, as visualized by UV light, was collected and freeze-dried. The sample was dissolved in water and loaded onto a Superose-12 gel filtration column (16 mm×500 mm, Amersham Pharmacia) equilibrated in 200 mM sodium phosphate buffer, pH 7.0. The column was eluted with 200 mM sodium phosphate buffer. The high molecular weight fluorescent fusion protein was separated from dissociated GFP and a small amount of other proteins with lower molecular weights. The fraction with the fluorescent fusion protein was purified further by HPLC with a semi-preparative polymeric reverse-phase column (10 μm PRP-1, 7×305 mm; Hamilton Co., Reno, NV, USA) as previously described (Zhao et al. 2002).

Glycosyl composition and linkage analysis

Neutral sugars were analyzed as alditol acetate derivatives by gas chromatography using a Hewlett-Packard HP-5 column (cross-linked 5% PH ME Siloxane, 30 m×0.32 mm×0.25 μm) programmed from 130 to 177°C at 1.2°C/min (Bhatti et al. 1970). Data were captured by Hewlett-Parkard ChemStation software. Purified GFP–AtAGP17 (100 μg) was used for each analysis with 50 nmol of myo-inositol as internal standard. Uronic acids of this glycoprotein (100 μg) were assayed by the colorimetric method based on the reaction with *m*-hydroxydiphenyl, using D-glucuronic acid as a standard (Blumenkrantz and Asboe-Hansen 1973). Linkage analysis was performed at the Complex Carbohydrate Research Center at the University of Georgia and at the Plant Cell Biology Research Centre at the University of Melbourne, as previously described (Kim and Carpita 1992, Merkle and Poppe 1994, Sims and Bacic 1995).

Chymotryptic digestion of GFP–AtAGP17 fusion protein

GFP was removed from the GFP–AtAGP17 fusion protein by chymotryptic digestion as described by Zhao et al. (2002) with minor modifications. Briefly, an aqueous solution with 5–10 mg of fusion protein was heat denatured in boiling water for 2 min, cooled and then incubated with a freshly prepared 0.01% (w/v) chymotrypsin solution with 2% (w/v) ammonium bicarbonate and 5 mM $CaCl_2$ for 24 h at room temperature. The sample was concentrated and subsequently fractionated with a Superose-12 gel filtration column and a PRP-1 column.

Amino acid composition analysis

Amino acid composition analysis of AtAGP17 without GFP (100 μg) was carried out by RP HPLC on a Beckman Gold System (Beckman Instruments Inc., Fullerton, CA, USA) after HCl hydrolysis and subsequent PITC (phenylisothiocyanate) derivatization, as described earlier (Bergman et al. 1986).

Co-precipitation with (β-D-galactosyl)$_3$ Yariv reagent

GFP–AtAGP17 fusion protein (50 or 100 μg) was dissolved in distilled water and precipitated by addition of an equal volume of (β-D-galactosyl)$_3$ Yariv reagent [1 mg ml^{-1} in 2% (w/v) NaCl aqueous solution] as described previously (Tan et al. 2003).

Hyp glycoside profiles

Purified GFP–AtAGP17 fusion protein (~10 mg) was hydrolyzed in 0.44 M sodium hydroxide (105°C, 18 h), neutralized, and fractionated on a C2 cation exchange column in order to elucidate the Hyp glycoside profile as described previously (Shpak et al. 1999).

RNA isolation and Northern blot analysis

Seedlings, cultured cells and different organs of 1-month-old *Arabidopsis* plants were ground with a mortar and pestle in liquid

nitrogen. Cauline and top rosette leaves were harvested as young leaves, while rosette leaves at the base of the plants were harvested as old leaves. Total RNA was extracted with the RNeasy Plant Total RNA kit (Qiagen, Chatsworth, CA, USA). RNA (10–20 μg) was electrophoresed in 1% agarose–formaldehyde gels and transferred by capillary action onto Zeta-Probe Genomic Tested Blotting Membranes following the manufacturer's recommendations (Bio-Rad, Hercules, CA, USA). DNA probes were labeled with [α-^{32}P]dCTP using the Prime-a-gene labeling system (Promega, Madison, WI, USA). Equivalent loading of RNA samples was confirmed by ethidium bromide staining of rRNA. RNA gel blots were hybridized with *AtAGP17*, *AtAGP18* and *AtAGP19* gene probes, corresponding to the complete coding regions without the signal peptides at 65°C in hybridization buffer (7% SDS, 0.25 M sodium phosphate, pH 7.2) overnight and washed at 65°C in 1 : 4 diluted hybridization buffer twice and 1 : 7 diluted hybridization buffer once. Washed membranes were exposed with Kodak storage phosphor screens (Kodak, Rochester, NY, USA). The hybridization intensity of specific mRNAs was scanned and quantified using a Personal Molecular Imager FX (Bio-Rad). Sizes of the hybridizing RNAs were determined by comparison with a set of RNA size markers run in the gel (Promega). Although *AtAGP17*, *AtAGP18* and *AtAGP19* gene sequences share sequence similarities, Northern blots show no cross-hybidization between probes. All three probes hybridize to unique and separable mRNAs species corresponding to different mRNA sizes predicted for these three genes.

Western blot analysis

The GFP–AtAGP17 fusion protein was separated by SDS–PAGE in 12% gels and subjected to Western blot analysis using an anti-GFP polyclonal antibody (BD Biosciences, San Diego, CA, USA) to detect the fusion protein, as described by Sun et al. (2004b).

Phylogenetic analysis

The protein sequences were downloaded from PubMed (http://www.pubmed.com). Alignment and phylogenetic analyses were performed using the Clustal X program (ftp://ftp-igbmc.u-strasbg.fr/pub/ClustalX/), and the phylogenetic tree was drawn using Treeview (http://taxonomy.zoology.gla.ac.uk/rod/treeview.html).

Acknowledgments

The authors thank Dr. Li Tan for assistance with Hyp glycoside profile analysis, Dr. Parastoo Azadi, Dr. Filomena Fettolino, Dr. Tony Bacic and Ms. Zofia Felton for glycosyl composition and linkage analyses, and Drs. Ivan Delgado and Ken Keegstra for providing *Arabidopsis* cell suspension cultures. This work was supported by National Science Foundation grants (IBN-9727757 and IBN-0110413) to A.M.S and M.J.K., by a Technology Action Fund grant to M.J.K. and Ohio University from the State of Ohio, and in part by the Department of Energy-funded (DE-FG02–93ER-20097) Center for Plant and Microbial Complex Carbohydrates.

References

Acosta-Garcia, G. and Vielle-Calzada, J.-P. (2004) A classical arabinogalactan protein is essential for the initiation of female gametogenesis in *Arabidopsis*. *Plant Cell* 16: 2614–2628.

An, G., Ebert, P.R., Mitra, A. and Ha, S.B. (1988) Binary vectors. *In* Plant Molecular Biology Manual. Edited by Gelvin, S.B and Schilperoort, R.A. pp. 1–19. Kluwer Academic Publishers, Dordrecht.

Arabidopsis Genome Initiative (2000) Analysis of the genome sequence of the flowering plant *Arabidopsis thaliana*. *Nature* 408: 796–815.

Aspinall, G.O. (1973) Carbohydrate polymers of plant cell walls. *In* Biogenesis of Plant Cell Wall Polysaccharides. Edited by Loewus, F. pp. 95–115. Academic Press, New York.

Bergman, T., Carlquist, M. and Jornvall, H. (1986) Amino acid analysis by high performance liquid chromatography of phenylthiocarbamyl derivatives. *In* Advanced Methods in Protein Microsequence Analysis. Edited by Wittmann-Liebold, B., Solnikow, J. and Erdmann, V.A. pp. 45–55. Springer-Verlag, Berlin.

Bhatti, T., Chambers, R.E. and Clamp, J.R. (1970) The gas chromatographic properties of biologically important N-acetylglucosamine derivatives, monosaccharides, disaccharides, trisaccharides, tetrasaccharides and pentasaccharides. *Biochim. Biophys. Acta* 222: 339–347.

Blumenkrantz, N. and Asboe-Hansen, G. (1973) New methods for quantitative determination of uronic acids. *Anal. Biochem.* 54: 484–489.

Borner, G.H.H., Lilley, K.S., Stevens, T.J. and Dupree, P. (2003) Identification of glycosylphosphatidylinositol-anchored proteins in *Arabidopsis*. A proteomic and genomic analysis. *Plant Physiol.* 132: 568–577.

Borner, G.H.H., Sherrier, D.J., Stevens, T.J., Arkin, I.T. and Dupree, P. (2002) Prediction of glycosylphosphatidylinositol (GPI)-anchored proteins in *Arabidopsis*: a genomic analysis. *Plant Physiol.* 129: 486–499.

Gao, M., Kieliszewski, M.J., Lamport, D.T.A. and Showalter, A.M. (1999) Isolation, characterization, and immunolocalization of a novel, modular tomato arabinogalactan-protein corresponding to the *LeAGP-1* gene. *Plant J.* 18: 43–56.

Gaspar, Y., Johnson, K.L., McKenna, J.A., Bacic, A. and Schultz, C.J. (2001) The complex structures of arabinogalactan-proteins and the journey towards understanding function. *Plant Mol. Biol.* 47: 161–176.

Gaspar, Y., Nam, J., Schultz, C.J., Lee, L.-Y., Gilson, P.R., Gelvin, S.B. and Bacic, A. (2004) Characterization of the *Arabidopsis* lysine-rich arabinogalactan-protein AtAGP17 mutant (*rat1*) that results in a decreased efficiency of *Agrobacterium* transformation. *Plant Physiol.* 135: 1–10.

Gilson, P., Gaspar, Y.M., Oxley, D., Youl, J.J. and Bacic, A. (2001) NaAGP4 is an arabinogalactan protein whose expression is suppressed by wounding and fungal infection in *Nicotiana alata*. *Protoplasma* 215: 128–139.

Goodrum, L.J., Patel, A., Leykam, J.F. and Kieliszewksi, M.J. (2000) Gum arabic glycoprotein contains glycomodules of both extensin and arabinogalactan-glycoproteins. *Phytochemistry* 54: 99–106.

Kieliszewski, M.J., Kamyab, A., Leykam, J.F. and Lamport, D.T.A. (1992) A histidine-rich extensin from *Zea mays* is an arabinogalactan protein. *Plant Physiol.* 99: 538–547.

Kieliszewski, M.J. and Lamport, D.T.A. (1994) Extensin: repetitive motifs, functional sites, post-translational codes and phylogeny. *Plant J.* 5: 157–172.

Kieliszewski, M.J., O'Neill, M., Leykam, J. and Orlando, R. (1995) Tandem mass spectrometry and structural elucidation of glycopeptides from a hydroxyproline-rich plant cell wall glycoprotein indicate that contiguous hydroxyproline residues are the major sites of hydroxyproline-O-arabinosylation. *J. Biol. Chem.* 270: 2541–2549.

Kim, J.-B. and Carpita, N.C. (1992) Changes in esterification of the uronic acid groups of cell wall polysaccharides during elongation of maize coleoptile. *Plant Physiol.* 98: 646–653.

Li, S. and Showalter, A.M. (1996) Cloning and developmental/stress-regulated expression of a gene encoding a tomato arabinogalactan protein. *Plant Mol. Biol.* 32: 641–652.

McCabe, P.F., Valentine, T.A., Forsberg, L.S. and Pennell, R.I. (1997) Soluble signals from cells identified at the cell wall establish a developmental pathway in carrot. *Plant Cell* 9: 2225–2241.

Merkle, R.K. and Poppe, I. (1994) Carbohydrate decomposition analysis of glycoconjugates by gas-liquid chromatography/mass spectrometry. *Methods Enzymol* 230: 1–15.

Merkouropoulos, G., Barnett, D.C. and Shirsat, A.H. (1999) The *Arabidopsis* extensin gene is developmentally regulated, is induced by wounding, methyl jasmonate, abscisic and salicylic acid, and codes for a protein with unusual motifs**.** *Planta* 208: 212–219.

Motose, H., Sugiyama, M. and Fukuda, H. (2004) A proteoglycan mediates inductive interaction during plant vascular development. *Nature* 429: 873–878.

Nam, J., Mysore, K.S., Zheng, C., Knue, M.K., Matthysse, A.G. and Gelvin, S.B. (1999) Identification of T-DNA tagged *Arabidopsis* mutants that are resistant to transformation by *Agrobacterium*. *Mol. Gen. Genet.* 261: 429–438.

Nothnagel, E.A. (1997) Proteoglycans and related components in plant cells. *Int. Rev. Cytol.* 174: 195–291.

Oxley, D. and Bacic, A. (1999) Structure of the glycosylphosphatidylinositol anchor of an arabinogalactan protein from *Pyrus communis* suspension-cultured cells. *Proc. Natl Acad. Sci. USA* 96: 14246–14251.

Park, M.H., Suzuki, Y., Chono, M., Knox, J.P. and Yamaguchi, I. (2003) CsAGP1, a gibberellin-responsive gene from cucumber hypocotyls, encodes a classical arabinogalactan protein and is involved in stem elongation. *Plant Physiol.* 131: 1450–1459.

Schultz, C.J., Rumsewicz, M.P., Johnson, K.L., Jones, B.J., Gaspar, Y.M. and Bacic, A. (2002) Using genomic resources to guide research directions. The arabinogalactan protein gene family as a test case. *Plant Physiol.* 129: 1448–1463.

Sherrier, D.J., Prime, T.A. and Dupree, P. (1999) Glycosylphosphatidylinositol-anchored cell-surface proteins from *Arabidopsis*. *Electrophoresis* 20: 2027–2035.

Shi, H., Kim, Y., Guo, Y., Stevenson, B. and Zhu, J.-K. (2003) The *Arabidopsis* SOS5 locus encodes a putative cell surface adhesion protein and is required for normal cell expansion. *Plant Cell* 15: 19–32.

Showalter, A.M. (2001) Arabinogalactan proteins: structure, expression and function. *Cell Mol. Life Sci.* 58: 1399–1417.

Shpak, E., Barbar, E., Leykam, J.F. and Kieliszewski, M.J. (2001) Contiguous hydroxyproline residues direct hydroxyproline arabinosylation in *Nicotiana tabacum*. *J. Biol. Chem.* 276: 11272–11278.

Shpak, E., Leykam, J.F. and Kieliszewski, M.J. (1999) Synthetic genes for glycoprotein design and the elucidation of hydroxyproline-O-glycosylation codes. *Proc. Natl Acad. Sci. USA* 96: 14736–14741.

Sims, I.M. and Bacic, A. (1995) Extracellular polysaccharides from suspension cultures of *Nicotiana plumbaginifolia*. *Phytochemistry* 38: 1397–1405.

Smith, J.J., Muldoon, E.P., Willard, J.J. and Lamport, D.T.A. (1986) Tomato *Lycopersicon esculentum* extensin precursors P-1 and P-2 are highly periodic structures. *Phytochemistry* 25: 1021–1030.

Sun, W., Kieliszewski, M.J. and Showalter A.M. (2004a) Overexpression of tomato LeAGP-1 arabinogalactan-protein promotes lateral branching and hampers reproductive development. *Plant J.* 40: 870–881.

Sun, W., Zhao, Z.D., Hare, M., Kieliszewski, M.J. and Showalter, A.M. (2004b) Tomato LeAGP-1 is a plasma membrane-bound, glycosylphosphatidylinositol-anchored arabinogalactan-protein. *Physiol. Plant.* 120: 319–327.

Svetek, J., Yadav, M.P. and Nothnagel, E.A. (1999) Presence of a glycosylphosphatidylinositol lipid anchor on rose arabinogalactan proteins. *J. Biol. Chem.* 274: 14724–14733.

Tan, L., Leykam, J.F. and Kieliszewski, M.J. (2003) Glycosylation motifs that direct arabinogalactan addition to arabinogalactan-proteins. *Plant Physiol.* 132: 1362–1369.

van Hengel, A.J. and Roberts, K. (2003) AtAGP30, an arabinogalactan-protein in the cell walls of the primary root, plays a role in root regeneration and seed germination. *Plant J.* 36: 256–270.

Youl, J.J., Bacic, A. and Oxley, D. (1998) Arabinogalactan-proteins from *Nicotiana alata* and *Pyrus communis* contain glycosylphosphatidylinositol membrane anchors. *Proc. Natl Acad. Sci. USA* 95: 7921–7926.

Zhang, Y., Brown, G., Whetten, R., Loopstra, C.A., Neale, D., Kieliszewski, M.J. and Sederoff, R.R. (2003) An arabinogalactan protein associated with secondary cell wall formation in differentiating xylem of loblolly pine. *Plant Mol. Biol.* 52: 91–102.

Zhao, Z.D., Tan, L., Showalter, A.M., Lamport, D.T.A. and Kieliszewski, M.J. (2002) Tomato LeAGP-1 arabinogalactan-protein purified from transgenic tobacco corroborates the Hyp contiguity hypothesis. *Plant J.* 31: 431–444.

(Received August 15, 2004; Accepted April 7, 2005)